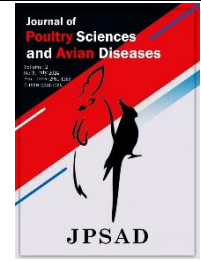





Journal of Poultry Sciences and Avian Diseases

Journal homepage: www.jpsad.com



Transcriptomic analysis of host immune response in the chickens infected by avian leukosis virus J using RNA-Seq



Paria Azamian¹, Saheb Foroutanifar^{1*}, Alireza Abdolmohammadi¹

¹ Department of Animal Science, Razi University, Kermanshah, Iran

* Corresponding author's email address: s.foroutanifar@razi.ac.ir

Article Info

Article type:

Original Paper

How to cite this article:

Azamian, P., Foroutanifar, S., & Abdolmohammadi, A. (2024). Transcriptomic analysis of host immune response in the chickens infected by avian leukosis virus J using RNA-Seq. *Journal of Poultry Sciences and Avian Diseases*, 2(3), 29-39.

<http://dx.doi.org/10.61838/kman.jpsad.2.3.3>



© 2024 the authors. Published by SANA AVIAN HOSPITAL, Tehran, Iran. This is an open-access article under the terms of the Creative Commons Attribution 4.0 International (CC BY 4.0) License.

ABSTRACT

The poultry's immune system is regulated by various genes involved in both innate and acquired immune responses. Understanding the changes in gene expression post-infection is essential for developing effective intervention strategies and improving disease management in the poultry industry. This study aimed to employ RNA-Seq to investigate the differential gene expression profiles and to identify the essential genes and pathways involved in the host response of poultry infected with the avian leukosis virus. For this purpose, RNA-Seq data of healthy and avian leukosis virus-infected birds on days 24 (n=6) and 40 (n=6) post-infection were used. After quality control and preprocessing, we aligned the reads to the chicken reference genome using STAR software and quantified gene expression using HTSeq-Count. Differential gene expression analysis was performed using the edgeR package in R. The results of this study showed that the uniquely mapped read percentage ranged from 78.07% to 87.74%, and the mismatch rate per base was found to vary between 0.77% and 1.45%. A total of 2,213 and 1165 genes exhibited significant differential expression compared to the control group on day 24 and 40 post-infection, respectively ($p < 0.05$). The gene ontology enrichment and pathway analysis revealed that six candidate genes, AvBD1, AvBD6, CATH1, CATH2, CATH3, and DEFB4A, are associated with the immune response on days 24 and 40. Additionally, on day 24, two more candidate genes, AvBD5 and LYG2, were found to be involved in the immune response.

Keywords: *Differential gene expression analysis, Immune system, Gallus Gallus, Avian leukosis viruses, RNA-seq.*

Article history:

Received 16 February 2024

Revised 26 May 2024

Accepted 10 June 2024

Published online 01 July 2024

1 Introduction

Avian diseases like avian influenza (AI), Newcastle disease (ND), infectious bursal disease (IBD), and avian leukosis viruses (ALVs) have a substantial adverse economic impact on the poultry industry globally. These diseases lead to significant economic losses due to mortality, decreased productivity, and trade restrictions imposed by various countries (1, 2). The outbreaks of these viral diseases result in the loss of birds, reduced production, job layoffs, and a decline in sales of poultry-related products like feeds, drugs, and equipment (1).

Avian leukosis viruses are classified into ten subgroups (A to J), with subgroups A, B, C, D, E, and J identified in chickens (2). ALV-J, discovered in broiler chickens since 1988, is associated with increased tumor formation, immune suppression, and higher mortality rates. Enhancing poultry resistance to ALV through genetic approaches and immune-related genes is crucial for disease-resistance breeding (3).

The poultry's immune system is regulated by various genes involved in both innate and acquired immune responses. Gene expression plays a crucial role in the immune response of poultry infected with the leukosis virus. Understanding the changes in gene expression post-infection is essential for developing effective intervention strategies and improving disease management in the poultry industry. Despite its importance, the molecular mechanisms underlying ALV infection and disease progression in poultry still need to be fully understood (4). Recent advances in high-throughput sequencing technologies, such as RNA sequencing (RNA-Seq), offer a powerful tool for profiling gene expression levels, identifying differentially expressed genes, and unraveling the complex regulatory networks underlying host-pathogen interactions (5). Studies have utilized RNA-Seq to analyze gene expression profiles, replacing traditional methods like microarrays (6, 7).

Identifying genes associated with the cellular immune response is crucial for enhancing immune responses in breeding programs, highlighting the significance of understanding the genetic mechanisms underlying immune regulation in poultry (8). RNA-Seq has been widely used to study the host-pathogen interaction and identify differentially expressed genes (DEGs) associated with various diseases, including viral infections (9). For example, RNA-Seq has been used to study the transcriptomic response of chickens to infectious bronchitis virus (10) and avian influenza virus (11). Sadr *et al.* (6) identified breed-specific DEGs, including those related to the immune system.

Truong *et al.* (12) further explored the role of DEGs in the spleen of chickens afflicted with necrotic enteritis, highlighting the potential for marker-based selection of disease-resistant chickens. Kumar *et al.* (13) expanded the scope of RNA-Seq analysis, identifying DEGs involved in acclimating Korean commercial chickens to different geographical locations. By analyzing the transcriptomic landscape of infected poultry tissues, we can gain insights into the molecular mechanisms driving the immune response and identify potential targets for therapeutic intervention. In this study, we employed RNA-Seq to investigate the differential gene expression profiles and to identify the key genes and pathways involved in the host response of poultry infected with ALV.

2 Materials and Methods

2.1 Sample collection and RNA extraction

The RNA-Seq data used in this study were retrieved from the European Nucleotide Archive (ENA) website (<https://www.ebi.ac.uk/ena>) under accession code ERP017744 (14). The data consisted of RNA-Seq reads from spleen samples of healthy and avian leukosis virus-infected birds. On the first day after hatching, ALV-challenged chicks were administered 100ul of SCDY1 Avian Leukosis Virus Subgroup J based on the TCID50 of the virus. Meanwhile, a control group was given 100ul of PBS per chick. Samples, including blood and immune organs, were collected from healthy and avian leukosis virus-infected birds on days 24 (n=6) and 40 (n=6) post-infection, respectively.

Total RNA was extracted from the spleen tissues using miRNeasy Mini kit (QIAGEN, Germany) in accordance with the manufacturer's protocol. The quality and quantity of the extracted RNA were evaluated using the NanoPhotometer spectrophotometer (Implen Inc., CA, USA). Only RNA samples with an RNA integrity number (RIN) ≥ 9.4 were used for further analysis. The RNA samples were then sequenced using a high-throughput sequencing platform to generate RNA-Seq data. The libraries were run on the Illumina HiSeq 2000 platform across six lanes, producing 100bp paired-end reads.

2.2 Quality control and preprocessing

Quality data assessment is a crucial step in differential gene expression (DGE) analysis to ensure the reliability and validity of the results. Several metrics are used to assess data

quality, including read quality scores, GC content, duplication rates, mapping rates, and gene expression levels. Low-quality reads, high GC content, excessive duplication, and poor mapping rates can introduce bias and errors into the analysis. We used FastQC software (version 0.10.1) (15) to evaluate the quality of our RNA-Seq data. The FastQC software generates an HTML file that displays the test results as graphs, with green (pass), orange (warning), or red (fail) marks indicating the status of each test. Additionally, the output file includes a table of basic statistics providing information about the data, such as the number of reads, read length, and GC content. The raw reads were then trimmed and filtered to remove adapters and low-quality bases using Trimmomatic (v0.39) (16).

3 Alignment to the reference genome

Trimmed RNA-seq reads were aligned to the reference genome using the STAR software (version 2.5.2a) (17). The STAR software requires three input files: the RNA-seq FASTQ data file, the reference genome of *Gallus gallus*, and a GTF annotation file. The reference genome and the GTF annotation files are publicly available on the Ensembl website. We carried out the alignment process individually for each data file in FASTQ format. This alignment process involved the alignment of reads to the reference genome, the generation of a SAM file containing the alignment information, and the conversion of the SAM file to a BAM file for further analysis. By aligning reads to the reference genome, we can determine the genomic locations from which the reads originated, allowing for the quantification of gene expression levels.

3.1 Quantification of gene expression

The aligned reads were counted using the HTSeq-Count software (version 0.6.1). This software takes the BAM file resulting from the STAR alignment and the GTF file as input and calculates the number of reads that overlap with the exons of each gene. The output of the HTSeq-Count software was a text file that contained the count data for each gene. This file was saved for further analysis, including differential gene expression analysis.

3.2 Differential gene expression analysis

We analyzed differential expression using the edgeR statistical package in R (version 3.6.1) (18) to estimate differential expression between two or more conditions

based on replicated samples' read counts. This package relies on a negative binomial distribution for modeling raw read counts at the gene level while adjusting for dispersion estimates based on the trend across all samples and genes. The input data for edgeR consisted of a matrix of read counts with row names corresponding to gene IDs and column names corresponding to sample IDs generated by HTSeq-Count software. The removal of genes that are unexpressed or very lowly expressed in the samples was done by computing the counts per gene per million mapped reads (cpm) and choosing a cutoff based on the median \log_2 -transformed cpm. To compare gene expression between two conditions, it is essential to calculate the ratio of reads assigned to each gene to the total number of reads. However, this calculation is complicated because RNA sequencing can vary between samples, and differences in read counts may be due to contaminations, biological reasons, or other systematic effects. To address these issues, we performed normalization to remove systematic effects unrelated to biological differences. The normalization method calculates a size factor for each sample, which is used to scale the count data. Gene-specific dispersion estimates are used to test for differential expression. Finally, differentially expressed genes between the infected and control samples were identified. We considered genes with an adjusted p -value < 0.05 cutoffs as differentially expressed.

3.3 Functional annotation and pathway analysis

To gain a more accurate and comprehensive understanding of the biological functions and processes of the differentially expressed genes, we performed functional annotation and pathway analysis. DAVID (Database for Annotation, Visualization, and Integrated Discovery) (19) was used to annotate and interpret the biological significance of differentially expressed genes with p -value < 0.05 and log-fold change higher than 2. DAVID is a web-accessible program to identify enriched biological pathways and processes that aid in interpreting datasets on a genomic scale, facilitating the transition from data collection to biological concepts.

4 Results and Discussion

4.1 RNA-Seq data quality assessment

In order to evaluate the overall quality of the sequencing data, we utilized the "per base sequence quality" metric as provided by FastQC. This comprehensive evaluation

involves summarizing data quality across ten distinct assessments, encompassing various factors critical for ensuring data integrity and reliability. The background plot of this test is divided into three regions. The green region indicates the desirable quality domain, the orange region indicates the acceptable quality domain and the red region indicates the undesirable and poor quality domain (15). According to the output plots, all the desired data were in the green region and the desirable quality domain (Figure 1).

This categorization within the green zone indicates high-quality sequencing data, suggesting that the sequences exhibit consistent quality across the bases. Specifically, this outcome suggests the minimal presence of base calls with low-quality scores, often the harbinger of sequencing errors or contaminations. Based on the basic statistics report for the data, for all data, the number of sequences flagged as poor quality was zero. The sequence length was 37, and the GC percentage was 48-49%.

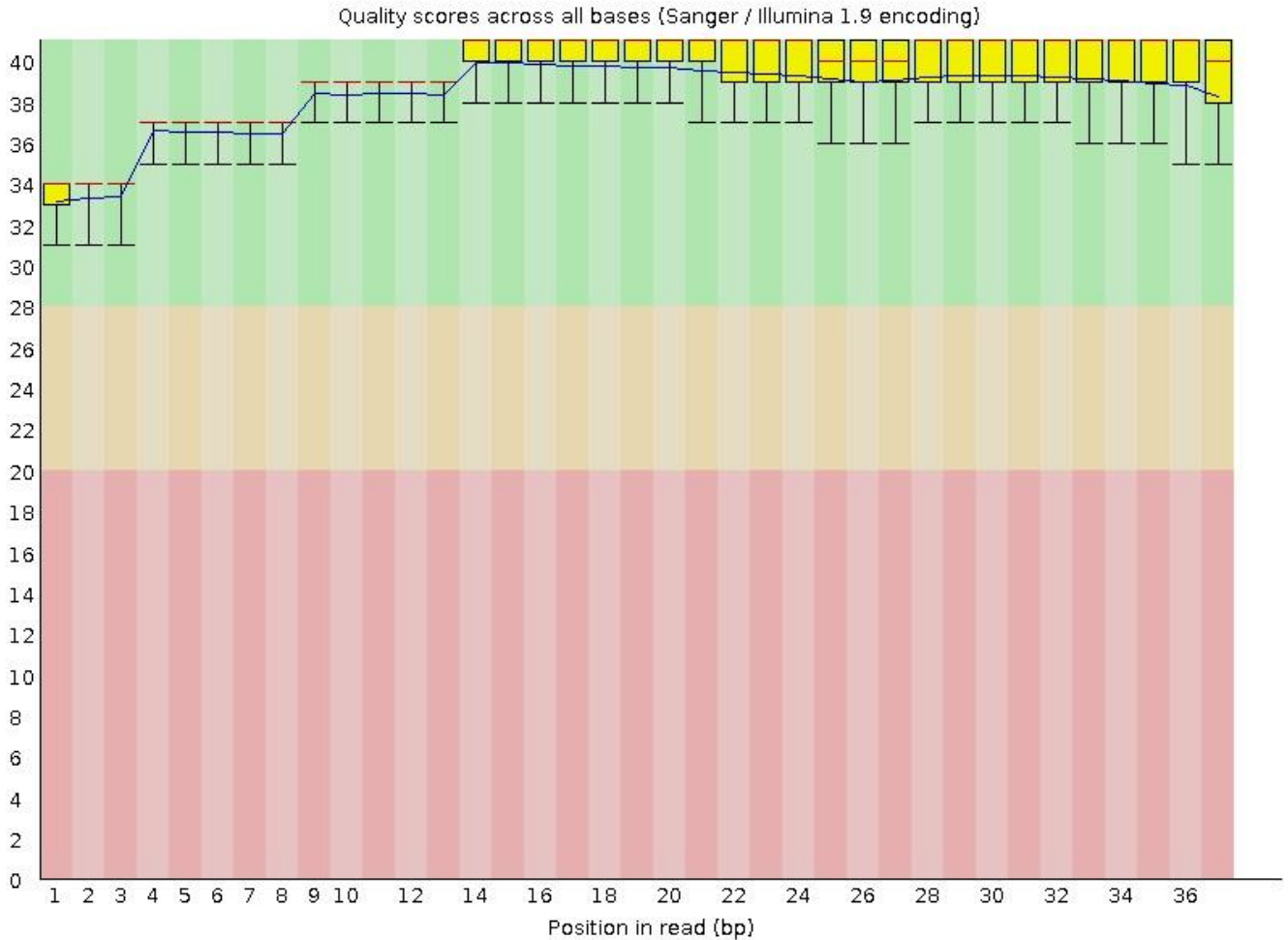


Figure 1. Per base sequence quality results from FastQC analysis.

4.2 Alignment Results and Mapping Statistics

The analysis of avian leukosis disease sequencing data yielded insightful metrics regarding the quality and effectiveness of the mapping process to the reference genome. The initial volume of input reads was substantial, averaging 69,046,919 reads per sample across the datasets considered.

STAR alignment results showed that an average of 58,106,442 reads per sample were successfully aligned to the

reference genome. Alignment efficiency, a pivotal metric of sequencing efficacy, was quantified as the proportion of uniquely mapped reads to the reference genome to total input reads (20). The uniquely mapped read percentage ranged from 78.07% to 87.74%, indicating a predominantly successful alignment process wherein most reads were precisely matched to specific genomic locations. This high mapping rate suggests that the sequencing data had a high level of coverage and depth and that the alignment process

effectively identified the correct genomic locations for the reads (6).

Another critical aspect of sequence analysis is the mismatch rate per base, which ranged between 0.77% and 1.45%. The mismatch rate measures the average number of mismatches at each nucleotide position and is an important indicator of the sequencing error rate (20). The observed mismatch rates are low, indicating high sequencing accuracy and a relatively low error rate.

The proportion of reads aligned to multiple locations was analyzed, revealing a range from 3.84% to 14.97%. Additionally, a small proportion of reads mapped to multiple locations on the reference genome indicates high specificity in the mapping process (12).

Given these metrics, it can be inferred that the homology mapping to the reference genome was executed proficiently. The substantial mapping rates coupled with low mismatch rates attest to the reliability and accuracy of the alignment process for the avian leukosis disease datasets.

4.3 Differential Gene Expression Analysis

To identify genes that were differentially expressed between the experimental and control groups, we used the EdgeR statistical package to analyze the RNA-Seq data. This comparison was meticulously designed to mirror the conditions under which the data were generated, ensuring an accurate reflection of the biological processes at play. The analysis revealed a significant number of genes that were differentially expressed between the control and virus-infected groups at both day 24 and day 40 after infection ($p < 0.05$). Our findings unveil a substantial alteration in gene expression patterns following viral infection. Specifically, on day 24 post-infection, a total of 2,213 genes exhibited significant differential expression compared to the control group ($p < 0.05$). Among these, 1,195 genes were upregulated, implying increased expression levels in response to the viral infection. This upregulation, indicative of enhanced gene activity in response to the viral infection, might suggest a reactive biological process or a compensatory mechanism triggered by the presence of the virus (21).

Conversely, a slightly larger subset of 1,018 genes was found to display decreased expression in the presence of the virus, signaling repression or downregulation of these genes in the infected state. This reduction in gene expression could reflect a direct consequence of viral infection on cellular functions or potentially signify a strategic viral evasion tactic undermining host defense mechanisms (12,21). At day 40, 1165 genes were identified as differentially expressed ($p < 0.05$), with 486 genes upregulated and 679 genes downregulated in the virus-infected group compared to the control group. A total of 796 of these genes were identical to genes with significant expression on day 24. Notably, the data demonstrated a marked disparity in the number of genes exhibiting altered expression levels at different time points post-infection. The number of differentially expressed genes was substantially higher on day 24 compared to day 40 following viral infection, suggesting that the virus infection had a more profound impact on the host transcriptome earlier. The differentially expressed genes are likely to play important roles in the host-pathogen interaction and may be involved in developing leukosis disease. Identifying these genes provides a valuable resource for further investigation into this disease's molecular mechanisms. Our results are consistent with Palmer's work, which also reported a substantial upregulation of immune-related genes at early time points following ALV-J infection in chickens (22, 23).

To visualize the differential expression patterns of these genes, we generated a heat map showing the logarithm of the read counts for genes with different expressions on days 24 and 40 after infection in different samples (Figure 2). The heat map reveals a clear separation between the control and infected groups, with distinct clusters of genes that are upregulated or downregulated in response to virus infection. The heat map's horizontal axis delineates the samples from both control and infected groups. In contrast, the vertical axis portrays the logarithm of the read counts pertinent to genes manifesting differential expression. These results provide a comprehensive view of the transcriptomic changes that occur in response to virus infection and highlight the importance of considering the temporal dynamics of gene expression in understanding the host-pathogen interaction.

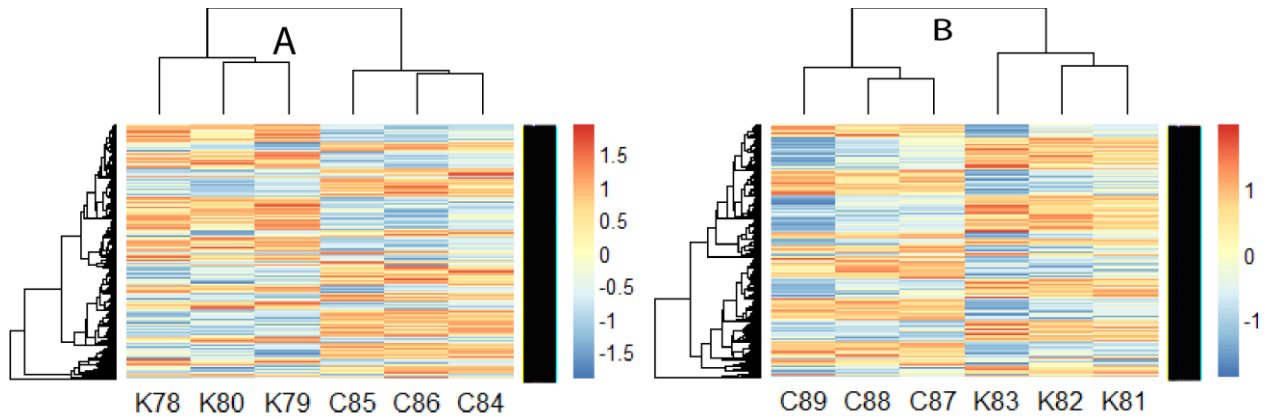


Figure 2. Hierarchical clustering and heat map of the logarithm of the read counts of the differentially expressed genes on days 24 (A) and 40 (B) after infection in different samples. C87, C88, and C89 represent control groups; k78, k79, and k80, infected groups. Red indicates a high expression level; blue indicates a low expression.

Our study's differential gene expression assessment was visually represented through an MA plot (Figure 3). Within this plot, each point corresponds to a gene, with the Y-axis (log ratio) reflecting the magnitude of expression difference and the X-axis (mean average) showcasing the average expression level across conditions. Our analysis revealed a distinct differential gene expression pattern, with many genes lying outside the threshold lines, indicative of substantial upregulation or downregulation. Among these, genes above the top threshold line were significantly

upregulated, whereas those below the bottom were markedly downregulated in the experimental group compared to the control group. A noteworthy feature of the MA plot was the symmetrical distribution of differentially expressed genes around the zero line of the Y-axis, underscoring the balanced nature of gene expression shifts between up and downregulation. This symmetry suggests that the cellular response to the condition under study involves a complex regulatory mechanism, affecting an extensive range of genes in both directions.

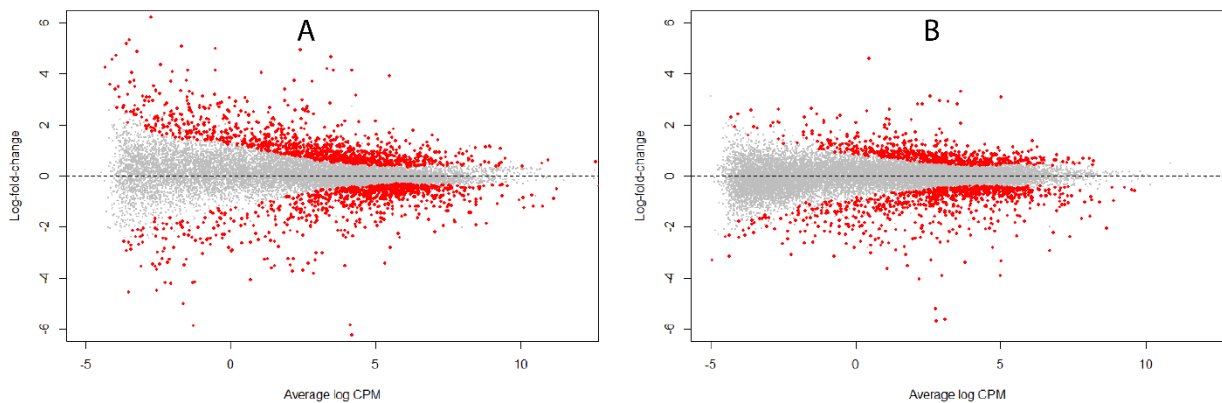


Figure 3. MA plot. Scatterplot of log₂ expression folds changes in infected versus control samples (y-axis) against the average expression level (x-axis). Genes with significant expression differences are shown in red, and gray points are not statistically significant genes.

4.4 Functional Annotation and Pathway Analysis

The differential gene expression analysis identified a subset of genes that exhibited significant changes in expression levels following poultry infection with leukosis virus. Then, we conducted a functional annotation analysis of these differentially expressed genes (DEGs) identified in poultry infected with the leukosis virus. Gene ontology (GO) enrichment analysis using the DAVID database was performed to elucidate the biological processes, molecular functions, and cellular components associated with the differentially expressed genes. Additionally, pathway analysis using the Kyoto Encyclopedia of Genes and Genomes (KEGG) databases was conducted to identify the biological pathways and networks enriched among the

differentially expressed genes. These analyses provide insights into the underlying biological mechanisms and pathways impacted by the viral infection, shedding light on the host response to the leukosis virus and potential therapeutic targets (24).

GO enrichment analysis revealed significant enrichment of biological processes, molecular functions, and cellular components among the DEGs, highlighting the diverse functional roles of the identified genes (Table 1). A diverse array of biological processes was enriched among the DEGs, with notable enrichment in immune-related processes such as innate immunity and immunity on days 24 and 40. Other enriched processes on day 24 included ion transport, neurogenesis, and transport, suggesting a multifaceted cellular response to leukosis virus infection.

Table 1. Enrichment of DGEs in biological processes identified through GO Analysis.

Day	Term	%	p-value	Genes
24	KW-0406~Ion transport	7.02	0.002	HCN4, RYR2, ASIC4, PGR2/3, GRIK1, GABRE, CACNG3, HCN1
24	KW-0399~Innate immunity	3.51	0.010	CATH1, C8B, CATH2, CATH3
24	KW-0524~Neurogenesis	2.63	0.080	NTRK2, MDGA1, MYT1
24	KW-0813~Transport	10.53	0.08	HCN4, RYR2, ASIC4, SLC6A13, PGR2/3, SLC6A11, HBE, GRIK1, GABRE, SCN2A, CACNG3, HCN1
40	KW-0399~Innate immunity	15.79	7.95E-4	CATH1, CATH2, CATH3
40	KW-0391~Immunity	15.79	0.006	CATH1, CATH2, CATH3

Molecular functions analysis identified enrichment in functions related to antimicrobial, antibiotic, and defending

on days 24 and 40, indicating the involvement of DEGs in the host defense reaction to the leukosis virus (Table 2).

Table 2. Enrichment of DGEs in molecular functions identified through GO Analysis.

Day	Term	%	p-value	Genes
24	KW-0929~Antimicrobial	7.02	1.04E-9	CATH1, AVBD5, AVBD6, AVBD1, LYG2, DEFB4A, CATH2, CATH3
24	KW-0044~Antibiotic	6.14	1.49E-8	CATH1, AVBD5, AVBD6, AVBD1, DEFB4A, CATH2, CATH3
24	KW-0211~Defensin	3.51	1.17E-4	AVBD5, AVBD6, AVBD1, DEFB4A
24	KW-0407~Ion channel	7.89	2.096E-4	HCN4, RYR2, ASIC4, PGR2/3, GRIK1, GABRE, SCN2A, CACNG3, HCN1
24	KW-1071~Ligand-gated ion channel	3.51	0.004	HCN4, RYR2, PGR2/3, HCN1
24	KW-0675~Receptor	11.40	0.055	NTRK2, IL5RA, PGR2/3, GRIK1, GRPR, ACVR2B, RXFP1, GFRA2, PRLHR2, GRM8, RHO, GPR158, DRD4
24	KW-0894~Sodium channel	1.75	0.08	HCN4, HCN1
40	KW-0044~Antibiotic	31.58	1.42E-10	CATH1, AVBD6, AVBD1, DEFB4A, CATH2, CATH3
40	KW-0929~Antimicrobial	31.58	3.79E-10	CATH1, AVBD6, AVBD1, DEFB4A, CATH2, CATH3
40	KW-0211~Defensin	15.79	1.95E-4	AVBD6, AVBD1, DEFB4A

Enrichment was also observed in molecular functions associated with ion channel, ligand-gated ion channel, receptor, and sodium channel on day 24, underscoring the regulatory roles of the identified genes in mediating intercellular communication and cellular signaling cascades.

Analysis of cellular components revealed enrichment in genes localized to the secreted cell membrane, cell junction, gap junction, and membrane, reflecting the diverse subcellular localization of proteins involved in host-virus interactions (Table 3).

Table 3. Enrichment of DGEs in cellular components identified through GO Analysis.

Day	Term	%	p-value	Genes
24	KW-0964~Secreted	15.79	1.18E-5	AVBD5, AVBD6, MYOC, NCAN, AVBD1, ASIP, IGF1, C8B, MMP9, CATH2, CATH3, DKK4, CATH1, OLFM1, FSTL5, GDF9, LYG2, DEFB4A
24	KW-1003~Cell membrane	14.03	0.023	NTRK2, SLC6A13, RXFP1, GFRA2, GJD2, GJB1, GJC2, GJB6, GRM8, LOC429249, GABRE, SCN2A, MDGA1, GPR158, CDH18, DRD4
24	KW-0965~Cell junction	3.51	0.059	GJD2, GJB1, GJC2, GJB6
24	KW-0303~Gap junction	1.75	0.0712	GJD2, GJB6
24	KW-0472~Membrane	42.98	0.088	RYR2, SLC35F4, IL5RA, GRIK1, GRPR, RXFP1, RGS5, GRM8, LOC420716, SLC6A13, SLC6A11, SEZ6L, UPK3A, GFRA2, GJD2, PRLHR2, CDH18, NLGN3, HCN4, RTN4R, SMIM5, LRMT2, LOC420903, ASIC4, DPP6, GJC2, GPNMB, PTPRZ1, RHO, LOC429249, GABRE, CACNG3, GPR158, DRD4, NTRK2, SUS2, PGR2/3, IGF1, TMEM196, ACVR2B, CATH3, LRFN5, GJB1, GJB6, GALNTL6, MDGA2, SCN2A, MDGA1, HCN1
40	KW-0964~Secreted	36.84	2.21E-5	GDF9, CATH1, AVBD6, AVBD1, DEFB4A, CATH2, CATH3

The findings of the current study indicate enrichment in molecular functions associated with ion channel, ligand-gated ion channel, receptor, and sodium channel on day 24 post-infection with Avian Leukosis Virus Subgroup J (ALV-J), highlighting the regulatory roles of the identified genes in mediating intercellular communication and cellular signaling cascades. Additionally, analysis of cellular components revealed enrichment in genes localized to the secreted cell membrane, cell junction, gap junction, and membrane, indicating the diverse subcellular localization of proteins involved in host-virus interactions. The enrichment of immune-related processes, particularly innate immunity, in our study underscores the critical role of the innate immune system in the early defense against ALV-J infection in poultry. The upregulation of genes involved in immune responses highlights the activation of host defense mechanisms to combat viral invasion and maintain homeostasis. These findings emphasize the significance of the host immune response in orchestrating the antiviral defense mechanisms during ALV-J infection. Our findings

align with the research by Feng *et al.*, who reported similar enrichment of immune-related processes, including upregulated genes involved in innate immunity and inflammatory responses in chickens infected with ALV-J (24, 25).

Pathway enrichment analysis using KEGG pathways identified two significantly enriched pathways associated with the DEGs, including the NOD-like receptor signaling pathway, shedding light on the molecular pathways perturbed during leukosis virus infection. Enrichment was observed in the Neuroactive ligand-receptor pathway on day 24, indicating the robust activation of immune responses in response to viral infection. These findings suggest that the leukosis virus infection triggers a robust immune response in poultry, highlighting their potential role in the underlying biological mechanisms (24). These results align with a study conducted by Chen *et al.*, which also found that the NOD-like receptor signaling pathway is activated by ALV-J infection in chickens (26).

Table 4. The candidate genes in the first cluster that are involved in the immune response

ID	Gene Name	Day
AvBD1	avian beta-defensin 1(AvBD1)	24 and 40
AvBD5	avian beta-defensin 5(AvBD5)	24
AvBD6	avian beta-defensin 6(AvBD6)	24 and 40
CATH1	cathelicidin-1(CATH1)	24 and 40
CATH2	cathelicidin-2(CATH2)	24 and 40
CATH3	cathelicidin-3(CATH3)	24 and 40
DEFB4A	defensin beta 4A(DEFB4A)	24 and 40
LYG2	lysozyme g2(LYG2)	24

We performed functional annotation clustering using the DAVID tool to identify functional modules among the DEGs. This analysis revealed significant enrichment in specific functional categories, identifying 13 and 3 clusters of genes with distinct biological functions on days 24 and 48 post-infection with Avian Leukosis Virus. Notably, the first cluster comprised 8 and 6 candidate genes associated with immune response, including those related to the NOD-like receptor signaling pathway (Table 4). Notably, genes such as AvBD1, AvBD6, CATH1, CATH2, CATH3, and DEFBA4 were implicated in immune responses on days 24 and 40, while AvBD5 and LYG2 genes were exclusively linked to immune responses on day 24. This cluster was significantly enriched in Gene Ontology (GO) terms related

to immune response, such as antimicrobial, antibiotic, defense response, defensin, and defense response to bacterium. By linking the differentially expressed genes to specific biological processes and pathways, we can better understand the host factors contributing to susceptibility or resistance to viral infection. These findings lay the groundwork for further investigations into the molecular pathways driving the host response to leukosis virus infection. Furthermore, integrating functional annotation and pathway analysis data with other omics technologies, such as proteomics and metabolomics, can provide a more comprehensive understanding of the molecular interactions underlying viral pathogenesis (6, 12).

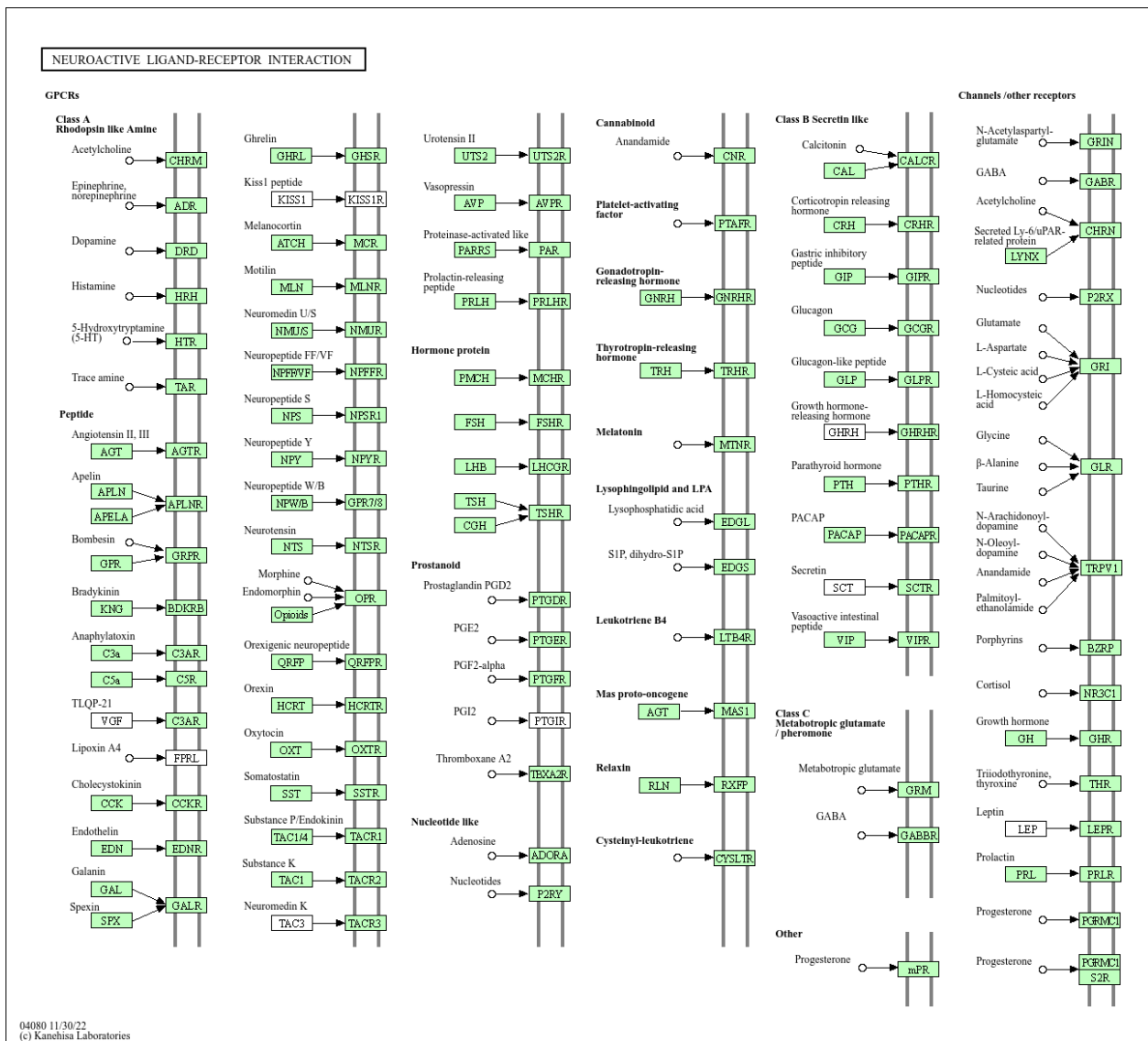


Figure 4. Neuroactive ligand-receptor pathway was identified using pathway enrichment analysis of DGEs using KEGG on day 24.

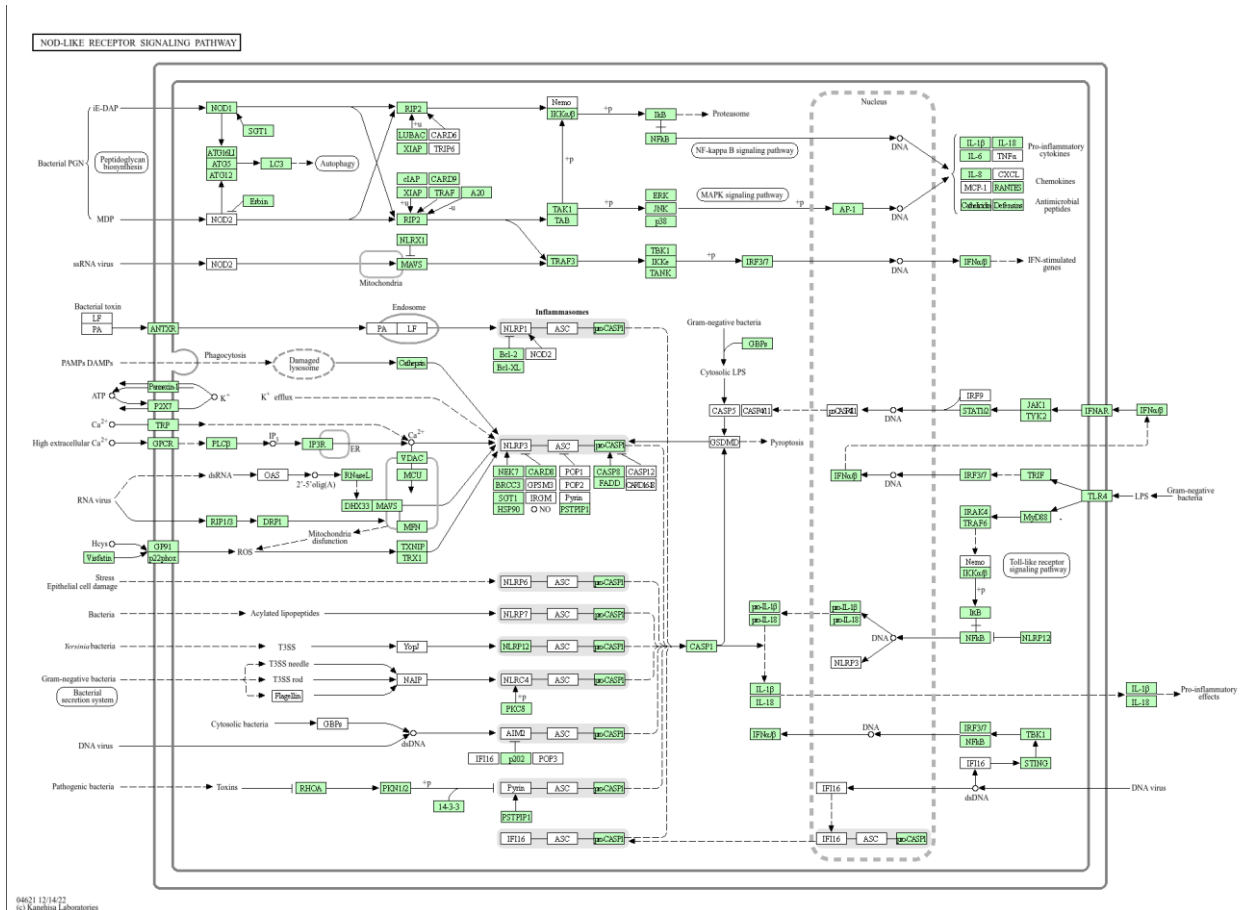


Figure 5. NOD-like receptor signaling pathway was identified using pathway enrichment analysis of DGEs Using KEGG on days 24 and 40.

5 Conclusion

In conclusion, the findings of the present study revealed significant differential expression of 2,213 and 1,165 genes on days 24 and 40, respectively, following infection with Avian Leukosis Virus Subgroup J. DAVID analysis revealed that a total of six candidate genes, AvBD1, AvBD6, CATH1, CATH2, CATH3, and DEFB4A, are associated with immune response on days 24 and 40. Additionally, on day 24, two more candidate genes, AvBD5 and LYG2, were found to be involved in the immune response. These genes were significantly enriched in Gene Ontology (GO) terms related to immune response, such as antimicrobial, antibiotic, defense response, defensin, and defense response to bacterium.

Acknowledgments

We thank deputy of research of the Razi University, for their support.

Conflict of Interest

The authors declare no conflicts of interest.

Author Contributions

S. F and P. A was responsible for formulating the project, developing critical conceptual ideas and handling most technical aspects. A. A authored the manuscript through collaborative discussions and edited it.

Data Availability Statement

Data are available from the corresponding author upon reasonable request.

Ethical Considerations

The Animal Care and Animal Handling rules and regulations, approved by the Animal Ethics Committee of

Razi University, were strictly followed for all live-animal-related procedures.

Funding

This study did not receive dedicated funding from any public, commercial, or not-for-profit organization.

References

- Fandiño S, Gomez-Lucia E, Benítez L, Doménech A. Avian leukosis: Will we be able to get rid of it? *Animals*. 2023;13(14):2358. [PMID: 37508135] [PMCID: PMC10376345] [DOI]
- Mo G, Wei P, Hu B, Nie Q, Zhang X. Advances on genetic and genomic studies of ALV resistance. *Journal of Animal Science and Biotechnology*. 2022;13(1):123. [PMID: 36217167] [PMCID: PMC9550310] [DOI]
- Wu L, Li Y, Chen X, Yang Y, Fang C, Gu Y, et al. Isolation and characterization of avian leukosis virus subgroup J associated with hemangioma and myelocytoma in layer chickens in China. *Frontiers in Veterinary Science*. 2022;9:970818. [PMID: 36246325] [PMCID: PMC9555167] [DOI]
- Wang M, Li H, Sun X, Qiu J, Jing C, Jia H, et al. J Subgroup Avian Leukosis Virus Strain Promotes Cell Proliferation by Negatively Regulating 14-3-3 σ Expressions in Chicken Fibroblast Cells. *Viruses*. 2023;15(2):404. [PMID: 36851618] [PMCID: PMC9960514] [DOI]
- Wang Z, Gerstein M, Snyder M. RNA-Seq: a revolutionary tool for transcriptomics. *Nature reviews genetics*. 2009;10(1):57-63. [PMID: 19015660] [PMCID: PMC2949280] [DOI]
- Sadr AS, Nassiri M, Ghaderi-Zefrehei M, Heidari M, Smith J, Muhaghegh Dolatabady M. RNA-Seq Profiling between Commercial and Indigenous Iranian Chickens Highlights Differences in Innate Immune Gene Expression. *Genes*. 2023;14(4):793. [PMID: 37107551] [PMCID: PMC10138050] [DOI]
- Zou M, Wang T, Wang Y, Luo R, Sun Y, Peng X. Comparative Transcriptome Analysis Reveals the Innate Immune Response to *Mycoplasma gallisepticum* Infection in Chicken Embryos and Newly Hatched Chicks. *Animals*. 2023;13(10):1667. [PMID: 37238096] [PMCID: PMC10215417] [DOI]
- Hammer D. The immune system in chickens. *Avian Pathology*. 1974;3(2):65-78. [PMID: 18777262] [DOI]
- Marioni JC, Mason CE, Mane SM, Stephens M, Gilad Y. RNA-seq: an assessment of technical reproducibility and comparison with gene expression arrays. *Genome research*. 2008;18(9):1509-17. [PMID: 18550803] [PMCID: PMC2527709] [DOI]
- Liu H, Yang X, Zhang Z, Li J, Zou W, Zeng F, et al. Comparative transcriptome analysis reveals induction of apoptosis in chicken kidney cells associated with the virulence of nephropathogenic infectious bronchitis virus. *Microbial pathogenesis*. 2017;113:451-9. [PMID: 29174688] [PMCID: PMC7126322] [DOI]
- Song H, Liu X, Gao X, Li J, Shang Y, Gao W, et al. Transcriptome analysis of pre-immune state induced by interferon-gamma inhibiting the replication of H9N2 avian influenza viruses in chicken embryo fibroblasts. *Infection, Genetics and Evolution*. 2022;103:105332. [PMID: 35811034] [DOI]
- Truong AD, Hong YH, Lillehoj HS. RNA-seq profiles of immune related genes in the spleen of necrotic enteritis-afflicted chicken lines. *Asian-Australasian journal of animal sciences*. 2015;28(10):1496. [PMID: 26323406] [PMCID: PMC4554858] [DOI]
- Kumar H, Choo H, Iskender AU, Srikanth K, Kim H, Zhunushov AT, et al. RNA seq analyses of chicken reveals biological pathways involved in acclimation into different geographical locations. *Scientific Reports*. 2020;10(1):19288. [PMID: 33159110] [PMCID: PMC7648748] [DOI]
- Lan X, Wang Y, Tian K, Ye F, Yin H, Zhao X, et al. Integrated host and viral transcriptome analyses reveal pathology and inflammatory response mechanisms to ALV-J injection in SPF chickens. *Scientific Reports*. 2017;7(1):46156. [PMID: 28401895] [PMCID: PMC5388866] [DOI]
- Andrews S. *FastQC: a quality control tool for high throughput sequence data*. Cambridge, United Kingdom; 2010.
- Bolger AM, Lohse M, Usadel B. Trimmomatic: a flexible trimmer for Illumina sequence data. *Bioinformatics*. 2014;30(15):2114-20. [PMID: 24695404] [PMCID: PMC4103590] [DOI]
- Dobin A, Davis CA, Schlesinger F, Drenkow J, Zaleski C, Jha S, et al. STAR: ultrafast universal RNA-seq aligner. *Bioinformatics*. 2013;29(1):15-21. [PMID: 23104886] [PMCID: PMC3530905] [DOI]
- Robinson MD, McCarthy DJ, Smyth GK. edgeR: a Bioconductor package for differential expression analysis of digital gene expression data. *bioinformatics*. 2010;26(1):139-40. [PMID: 19910308] [PMCID: PMC2796818] [DOI]
- Dennis G, Sherman BT, Hosack DA, Yang J, Gao W, Lane HC, et al. DAVID: database for annotation, visualization, and integrated discovery. *Genome biology*. 2003;4:1-11. [DOI]
- Langmead B, Trapnell C, Pop M, Salzberg SL. Ultrafast and memory-efficient alignment of short DNA sequences to the human genome. *Genome biology*. 2009;10:1-10. [PMID: 19261174] [PMCID: PMC2690996] [DOI]
- Wang Y, Lupiani B, Reddy S, Lamont SJ, Zhou H. RNA-seq analysis revealed novel genes and signaling pathway associated with disease resistance to avian influenza virus infection in chickens. *Poultry science*. 2014;93(2):485-93. [DOI]
- Palmer CS. Innate metabolic responses against viral infections. *Nature Metabolism*. 2022;4(10):1245-59. [PMID: 36266542] [DOI]
- Hang B, Sang J, Qin A, Qian K, Shao H, Mei M, et al. Transcription analysis of the response of chicken bursa of Fabricius to avian leukosis virus subgroup J strain JS09GY3. *Virus research*. 2014;188:8-14. [PMID: 24680656] [DOI]
- Qiu L, Chang G, Li Z, Bi Y, Liu X, Chen G. Comprehensive transcriptome analysis reveals competing endogenous RNA networks during avian leukosis virus, subgroup j-induced tumorigenesis in chickens. *Frontiers in Physiology*. 2018;9:996. [PMID: 30093865] [PMCID: PMC6070742] [DOI]
- Feng M, Dai M, Xie T, Li Z, Shi M, Zhang X. Innate immune responses in ALV-J infected chicks and chickens with hemangioma in vivo. *Frontiers in microbiology*. 2016;7:786. [DOI]
- Chen G, Li Z, Su S, Chang G, Qiu L, Zhu P, et al. Identification of key genes fluctuated induced by avian leukemia virus (ALV-J) infection in chicken cells. *In Vitro Cellular & Developmental Biology-Animal*. 2018;54:41-51. [PMID: 29197030] [DOI]